
NETWORK MODELLING IN ANALYSING CYBER-RELATED GRAPHS

A PREPRINT

Vesa Kuikka^[0000–0002–3677–816X]
Department of Computer Science
Aalto University School of Science
Finland
vesa.kuikka@aalto.fi

Lauri Pykälä
Department of Computer Science
Aalto University School of Science
Finland

Tuomas Takko
Department of Computer Science
Aalto University School of Science
Finland

Kimmo K. Kaski^[0000–0002–3805–9687]
Department of Computer Science
Aalto University School of Science
Finland

December 20, 2024

ABSTRACT

In order to improve the resilience of computer infrastructure against cyber attacks and finding ways to mitigate their impact we need to understand their structure and dynamics. Here we propose a novel network-based influence spreading model to investigate event trajectories or paths in various types of attack and causal graphs, which can be directed, weighted, and / or cyclic. In case of attack graphs with acyclic paths, only self-avoiding attack chains are allowed. In the framework of our model a detailed probabilistic analysis beyond the traditional visualisation of attack graphs, based on vulnerabilities, services, and exploitabilities, can be performed. In order to demonstrate the capabilities of the model, we present three use cases with cyber-related graphs, namely two attack graphs and a causal graph. The model can be of benefit to cyber analysts in generating quantitative metrics for prioritisation, summaries, or analysis of larger graphs.

Keywords Attack modelling technique · Network modelling · Attack graph · Causal graph · Directed acyclic graph

1 Introduction

Cyber-attacks are unauthorised actions against computer infrastructure to exploit vulnerabilities in the target systems and a cyber threat refers to a potential adversarial event in which an attacker could exploit vulnerabilities [14]. Typically, a cyber attack can consist of a number of actions, events, or steps required for the attacker to gain access or sufficient privileges to achieve the objective of the attack, e.g. denial of service (DOS) or the delivery and use of malware. A common approach to classifying these steps has been through various frameworks such as the cyber kill chain [7]. At a more technical level, potential or real cyber attacks have often been modelled as directed graph structures. Among these graph-based methods, attack graphs and their variants are commonly used to represent cyber-attacks. [12, 25, 15] There are two commonly used forms of attack graphs: the first is a directed graph with nodes representing network states and edges representing exploits, while the second uses nodes to represent pre- or post-conditions of an exploit and edges to show the consequences. In addition, knowledge-based methods are used to model attack concepts and vulnerability details [4, 17, 20].

In order to understand, analyse, and visualise the sequence of events of a successful cyber attack, we will here use attack modelling techniques (AMTs). There are three main categories of AMT: (i) methods based on use cases like misuse

or security use cases, (ii) temporal methods based on e.g. cyber kill chains, and (iii) methods based on graphs [12]. Here we will focus on graph-based models as they enable analysts and researchers to formulate and use different metrics, both quantitative and qualitative, for optimising and prioritisation of defensive efforts [12]. The graph-based cyber attack modelling can be performed at various technological levels, such as the levels of applications, services or whole computer networks. For this mappings from technical micro-service levels to higher aggregation levels can be accomplished with the help of technical configuration repositories.

In the literature, the term *attack graph* has been used to refer to a variety of modelling approaches. Ref. [23] presents an overall taxonomy of these models based on the analysis of 70 different attack graph formalisms. This taxonomy uses a hierarchical categorisation system with two top-level categories: sequential models and causal dependency models. Sequential models represent attack steps or paths, while causal dependency models focus on cause-effect relationships. The authors further categorise sequential models, based on node semantics, into asset-oriented, vulnerability/exploit-oriented, and condition/attribute-oriented types.

Our proposed approach will be based on network modelling as it offers various tools for analysing cyber-related graphs from different perspectives and aggregation levels. The method consists of modelling the network structure and network flow on a detailed node and link level. [10, 2, 11] The network model applies to Markov processes and utilises probability theory [24] to calculate combined effects from multiple sources.

In this study, we present the modelling of cyber-related graphs through three use cases and illustrate how the model can be utilised to examine exploitability, causality, and incomplete graph information. The first use case [21] involves a directed acyclic graph in which the states of the system are represented as nodes and vulnerabilities as links between the nodes, forming an attack graph. The exploitability of a vulnerability is interpreted as the probability of a successful exploit (ie. traversability of a link). In the network model, these probabilities are assigned to link weights. The second use case demonstrates a larger network structure of services and applications [3], which with the first use case demonstrate how the exploitability metrics can be used to assign weights to individual links in the graph. The third use case involves two types of nodes, namely attack entities and non-attack entities identified by an attack investigation tool using natural language processing and deep learning [3, 5].

These use cases illustrate how different categorisations can be utilised in the model. Since the metrics of the model are presented as probabilities, they can help us to form a consistent understanding of the situation from different perspectives. Our proposed method introduces novel features for analysing cyber-related graphs, including acyclic and cyclic paths. It uses a detailed model to consider all accessible paths through the nodes of the network and defines new metrics to estimate the exploitability and impacts. For example, the model can be used to calculate the effects of removing a specific vulnerability or protecting a service in the system.

In Section 2, we will present our network modelling methods and analysis metrics. Detailed algorithms will not be included in this study, as they have previously been published. In Section 3, we describe the data and networks of the use cases on which the model is demonstrated with. In Section 4, we will explain how the model can be used to obtain new results in analysing cyber-related graphs through the three use cases. In Section 5, we will discuss the applications of our graph-based methods in analysing cyber vulnerabilities and attacks, and present concluding remarks.

2 Attack Graph Model

Graphs related to cyber security, such as attack graphs and causal graphs, are primarily created for cyber security experts to help them understand the sequence of an attack and plan ways to prevent it. These graphs are usually generated from large volumes of data for this purpose [19, 22]. Consequently, the resulting graphs typically contain a small number of nodes, ranging from a few to hundreds.

Our network modelling methods [11] consider various aspects to analyse cyber attack processes and prioritise preventive or mitigation actions [6, 18] against potential or ongoing cyber attacks. The model describes the network structure, including individual nodes and links. Influence spreads through a non-conserved process, moving from a node to all neighbouring nodes via directed links. The network model described in [11] was created for influence spreading and it can be used to examine both acyclic or cyclic Markov processes on complex network structures. However, in this study, the model is used to describe attack propagation along self-avoiding paths, which is better suited for modelling attack propagation along acyclic paths. The weights assigned to directed links describe the probabilities of successful propagation steps of an attack in a graph structure.

This model offers different approaches for dealing with the full breakthrough of nodes or self-avoiding paths. The first approach permits loops in the spreading process, while the second approach is better for examining connectivity between nodes. Loops consist of a minimum of three nodes connected by links, enabling circular propagation of influence within the network structure. Both methods yield similar results for directed acyclic graphs due to the network

lacking cyclic processes. In the case of full breakthrough effects, a bidirectional link leads to a cyclic process between the two nodes at each end of the link, where bidirectional links cause recurring events between two nodes in the network. Note that due to the spreading, the effects are not limited to those nodes but spread throughout the network structure. In the case of self-avoiding paths, no recurring effects are permitted, and the process can only propagate in one direction along a path.

The method and corresponding algorithms proposed in our earlier articles [11] are based on modelling network structure and spreading processes. This results in an $N \times N$ probability matrix C , where the number of nodes in the network is denoted by N . The matrix elements represent directed spreading or connectivity probabilities between all node pairs in the network with a connecting path between them. Subsequently, this matrix is used to define various metrics for analysing the network structure and network flow process. Note that models other than our influence spreading model can also be used to generate the probability matrix. As the analysis is based on the probability matrix, it is independent of the method used to produce the matrix. These models could even be non-Markovian or include other event types besides mutually non-exclusive events (OR rule) used to combine multiple joining alternative paths [11]).

In network analysis, we use two metrics to evaluate the importance of a node, namely out-centrality and in-centrality, and they are defined differently from the standard closeness centrality measures in the literature. One reason for using different metrics is the limitations of standard metrics in describing detailed network structures, due to being defined based on the shortest paths between nodes thus ignoring other alternative paths [13]. We use the probability matrix as a basis for analysis, as it enables the separation of the network modelling from the analysis [11].

Next we define the centrality measures for the subset of nodes V in the network G of N nodes. (Note that in the case of entire network $V=G$). For the influence spreading through the network we define the out-centrality of source node s by

$$C^{(\text{out})}(s) = \frac{1}{N-1} \sum_{\substack{t \in V \\ s \neq t}} C(s, t) \quad (1)$$

and the in-centrality of a target node t by

$$C^{(\text{in})}(t) = \frac{1}{N-1} \sum_{\substack{s \in V \\ s \neq t}} C(s, t). \quad (2)$$

Here the out-centrality of a node is the average value of probabilities of spreading from the source node to all other nodes in V , while the in-centrality of a node is the average value of probabilities of spreading from all other nodes in V to the target node. These centrality measures describe physical properties of the network structure and flow process. As $C(s, t)$ is the probability of influence spreading from node s to node t , the sum in Eq. 1 is interpreted as an expected value of influenced nodes and the sum in Eq. 2 as the expected number of nodes that spread influence to the specified node. In the context of cyber-related graphs, influence spreading refers to the propagation of cyber attacks within the graph. In this study, we adopt the convention of setting the initial value of the source node as zero and using the corresponding normalisation factor $1/(N-1)$ and express the results as percentage values.

When dealing with cyber-related graphs, the out-centrality is a measure for assessing the potential effect of a cyber attack on other nodes within the network. On the other hand, the in-centrality is useful for understanding how various cyber attacks can affect nodes in the network. Detailed information can be obtained by focusing on a subset of start and end nodes using Eqs. 1 and 2. Typically, the main focus is to explore the vulnerability and the effect of a start node on an end node. Multiple start nodes and end nodes can exist in one cyber-related graph.

We work with numerical quantities for the exploitability and impact information. The exploitability represents the probability of a successful cyber attack through a link, while the impact describes the effect on the system, functionality, or operation. To assess the impact of different needs on both the technical and operational levels, the first step is to define the concept in the specific situation and need. The impact is calculated for the nodes, and the exploitability is calculated for the links. We assume that the impact value does not influence the probabilities of cyber attack propagation. Therefore, the impact values may not be expressed as probabilities and can have numerical values beyond the $[0, 1]$ range. However, the impact values for different nodes are comparable, enabling us to calculate the desired sums for paths or network structures.

Our approach is based on using link weights as probabilities to represent successful exploits. The exploitability metric measures the current state of exploit techniques or code availability. When easily accessible exploit code is publicly available, it increases the number of potential attackers, including unskilled ones, which in turn increases the severity of the vulnerability. The following equation illustrates how the factors *AccessVector*, *AccessComplexity*, and *Authentication* explain the accessibility and complexity of the vulnerability, and whether additional conditions are

needed to exploit it. The exploitability metric is defined as follows [16]:

$$\text{Exploitability} = 20 * \text{AccessVector} * \text{AccessComplexity} * \text{Authentication}. \quad (3)$$

Impact metrics measure how a vulnerability, if exploited, will directly affect an IT asset. These impacts are independently defined as the degree of loss of confidentiality, integrity, and availability. The total impact metric is defined as [16]:

$$\text{Impact} = 10.41 * (1 - (1 - \text{ConfImpact}) * (1 - \text{IntegImpact}) * (1 - \text{AvailImpact})). \quad (4)$$

In a network structure, a node can be targeted by different cyber attack paths from the source node through various links directed to the target node. In an attack graph, these may involve the same vulnerability. However, if different vulnerabilities can be exploited on one node, we calculate the weighted average value for the node or use the maximum impact of alternative exploits. We define a vector I with elements representing the impact values for the nodes in the network. The impact of a cyber attack from the start nodes S to the end nodes T can be defined as:

$$\mathcal{I}(S, T; I) = \frac{1}{N-1} \sum_{\substack{i \in S \\ j \in T}} C_{i,j} I_j, \quad (5)$$

where the matrix C consist of elements $C(i, j)$ that represent the probabilities of successful attacks from node i to node j via alternative paths. The impact value on the end node alone includes the last exploit on the path. The impact value of Eq. 5 can be calculated for specific events, such as the impact on particular services. Additionally, Eq. 5 can be utilised to analyse the impact of exploits by determining the decrease in the impact value after mitigating vulnerabilities.

When all elements of vector I are set to one, we obtain a quantity that describes the attack propagation from the source node set S to the target node set T in the network. In this way, the impact value in Eq. 5 is linked to the out- and in-centrality metrics in Eqs. 1 and 2. Therefore, the centrality measures and the impact measure in Eq. 5 are defined consistently with each other. Combining the alternative paths using probabilistic methods allows us to calculate metrics based on Eqs. 3 and 4 for real-world cyber attacks and different categorisations.

The cumulative impact for individual paths has been analysed in [21]. In our model, the cumulative impact along a path is calculated by summing up the products of propagation probabilities and node impacts according to Eq. 5. Once again, the impact on the end node only includes the impact on that node.

In summary, four kinds of impact metrics can be calculated: cumulative impacts along individual paths or all alternative paths, and the impact on end nodes through individual or all alternative paths. In this study, we prefer metrics that combine alternative paths using probability theory methods. The factors $C_{i,j}$ in Eq. 5 account for the effects of all potential alternative paths. This approach allows for the definition of new metrics in analysing cyber events from different perspectives and categorisations. In the next section we provide examples of this as use cases.

3 Use Case Data

For this study we choose three different graph structures, described in Table 1 to serve as our use cases.

Table 1: Summary of the use case graphs.

Graph	Description	Nodes	Links	Reference
Multi-cloud Enterprise Network	Netflix OSS microservice system	18	25	[21]
Netflix OSS	Netflix OSS microservice system	21	94	[21]
ATLAS, Pony campaign attack	Recovered sequences and a causal graph	39	65	[3, 5]

Use case 1: Multi-cloud Enterprise Network. The graph for the Multi-cloud Enterprise network from [21] represents the network topology of two cloud infrastructures connected to the Internet behind an external firewall. The first cloud server hosts three virtual machines, all connected to a virtual switch. The second cloud server hosts a public network and a private network. External users can access a web server, and internal users can access the SQL server from inside the local network. Each server in this topology represents a realistic vendor-specific system with a set of real-world CVE vulnerabilities, with the impacts of exploitation extracted from the CVE database.

Use case 2: Netflix OSS Architecture. [8] used a combination of tools to construct attack graphs for microservice architectures, consisting of a Docker host running various interconnected containers. The network topology was extracted from the docker-compose configuration files that define the orchestration of the services and details about the connections between containers, published ports, and any privileged access granted to containers. Vulnerabilities were scanned from the Docker images using the vulnerability scanning software Clair, producing a list of CVEs with textual descriptions and attack vectors for each image. The topology and vulnerability data were used as input for the final attack graph generation process. Attack pre-and postcondition parsing was performed by matching the attack vectors of the vulnerabilities by keyword matching [1].

Use case 3: Pony APT campaign. In the research conducted on the Pony APT campaign (CVE-2017-0199) [5], the methodology was based on the work by [3], describing a framework for constructing "attack stories" from audit logs. Their approach involved several steps. First, a platform-independent causal graph representation was constructed using various system audit logs, including DNS records, web objects, processes, file accesses, and network connections. This graph was then abstracted using optimisation techniques to reduce its complexity. Specifically, nodes and edges that were not reachable from the attack nodes or attack symptom nodes were removed, repeated edges between entities were reduced to only the first occurrence, and nodes and edges referring to the same type of event were combined.

Next, the process of attack sequence construction took place. All "attack entities" from the causal graph were obtained, and subsets consisting of two or more attack entities were formed. The neighbourhood graph for each entity within these subsets was extracted, followed by retrieving time-stamped events for each neighbourhood graph. Sequences were labelled attack sequences if they consisted exclusively of attack events, which means that both the source and destination nodes were associated with attacks. Following this, sequence lemmatisation was performed. This involved transforming sequences into a textual representation using a general vocabulary of 30 words, divided into four types: process, file, network, and actions. To balance the dataset, non-attack sequences were undersampled, and attack sequences were oversampled by mutating existing attack sequences. Finally, the sequences were embedded and modelled, followed by an investigation of attack and recovery of "attack stories". In the resulting processed graph, the semantic interpretations of nodes and edges are connected to system states inferred from the audit logs. The nodes represent processes (i.e. executables), files or IP addresses. The edges between them in turn represent actions or events between the entities, like read, write, execute, or connect.

The ATLAS approach thus focuses on reconstructing the attack story from observed system behaviours, with nodes and edges closely tied to actual system events and entities as recorded in the audit logs. Currently, the calculations treat all nodes in the graph equivalently, even in the use case where the graph nodes represent different entity types. A potential direction for further study is to treat different entities in the multiplex graph as distinct and perform the calculations separately for each node class.

4 Results

In this section, we show the results of our attack graph model for three different use cases. The first use case presents a small directed acyclic attack graph. [21] The second use case is a more complex attack graph from [21] and finally the third use case is an attack graph that was generated by an attack investigation tool using natural language processing and deep learning [3].

Use Case 1: Multi-cloud Enterprise Network. We use a multi-cloud enterprise network as the first use case to demonstrate our modelling method. The network topology and vulnerabilities are adopted from [21]. The first cloud server hosts three virtual machines: a Mail server, a Web server, and a DNS server, and the second cloud server consists of public and private networks. The public network hosts an SQL server and a NAT gateway server, and the private network hosts an Admin server and three virtual machines (VMs). Users outside the network can access the Web server, and employees within the same LAN can access the SQL server through their workstations.

Fig. 1 shows the attack graph on the Multi-cloud Enterprise Network that consists of directed links representing the exploits and nodes the states. These kinds of networks are directed acyclic graphs (DAGs), i.e. without cycles [9].

The systems have vulnerabilities that are listed in the CVE vulnerabilities database. [16] The attacker's goal is to compromise a virtual machine in the private network or the database in the public network by gaining root access. The attacker can take different paths in the attack graph.

In Table 2 we show the impact and exploitability values calculated for vulnerabilities in the attack graph (Fig. 1). The third column of this table shows the list of links in the attack graph for each vulnerability. In Fig. 2 we depict the non-cumulative impact values of successful cyber attacks from the start node 1 to other nodes in the graph. For example, the node 7 has a lower impact than nodes 6, 14, and 17 because the vulnerability CVE-2007-4752 from the start node

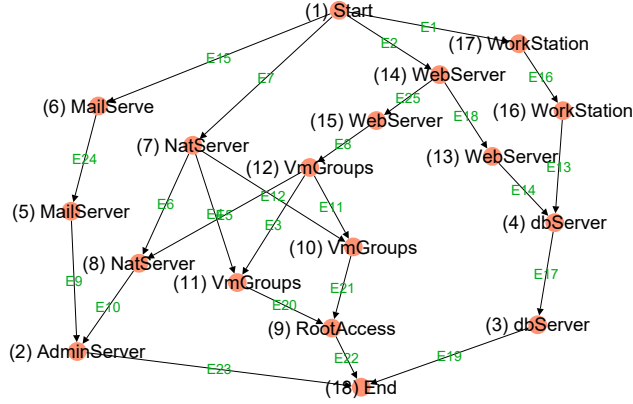


Figure 1: Use Case 1: Attack graph Multi-cloud Enterprise Network [21].

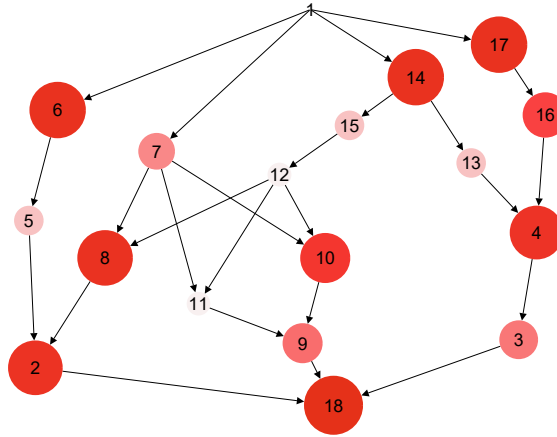


Figure 2: Impacts of successful cyber attacks from the start node 1 of Fig. 1 to other nodes in the graph. The node size and colour describe the exploitability and impact factors (see Eq. 5).

to node 7 has a relatively low impact value. On the other hand, the node 10 has a high impact value, because the vulnerability CVE-2008-0015 from nodes 7 and 12 to node 10 has a high impact value. The effects on other end nodes can be reasoned similarly according to Eq. 5.

In our model, we use out-centrality and in-centrality metrics to analyse the propagation of attacks from potential start nodes to potential end nodes. In Fig. 1, node 1 is the start node and node 18 is the end node, but there could be other nodes where the attack chain can start or end. For example, let us consider database servers (dbServer) as the attacker's goal, like in [21]. Eqs. 1 and 2 define out-centrality and in-centrality metrics as average values over the whole network structure, not just for possible start and end nodes. There are a few reasons for this. Initially, the start and end nodes might change depending on the situation, or this information may not be available. Furthermore, complete metric data provide details about the structure of the attack graph, which can be used to plan mitigation actions against unknown attack scenarios. In addition, it is straightforward to define metrics for a subset of start nodes and a subset of end nodes similarly to Eq. 5.

The out-centrality (Eq. 1) and in-centrality (Eq. 2) values for the 18 nodes of the Multi-cloud network are shown in Fig. 3. The results are shown for the four link weight values $w = 0.2, 0.5, 0.8,$ and 1 . As the link weights are interpreted as probabilities of successful exploitation of vulnerabilities, lower link weight values correspond to reduced probabilities.

The out-centrality and in-centrality values depicted in Fig. 3 illustrate the typical characteristics of directed acyclic networks. Node 1 (Start) has the highest out-centrality, while node 18 (End) has the highest in-centrality. The out-centrality values tend to be more varied than the in-centrality values, as structures near the source nodes and high link weights boost propagation more than structures near target nodes. We also observe that the number of potential alternative paths affects the out-centrality and in-centrality values. Nodes 7, 12, 14, and 15 have high out-centrality

Table 2: Exploitability and impact values calculated from Eqs. 3 and 4 for vulnerabilities in the attack graph of Fig. 1 [21].

Vulnerability	Exploitability/10	Impact	Links
-	1	-	E1, E2
CVE-2010-3847	0.339258	10.00085	E3, E4, E20
CVE-2003-0693	0.99968	10.00085	E5, E6
CVE-2007-4752	0.99968	6.442977	E7
CVE-2001-0439	0.99968	6.442977	E8
CVE-2008-4050	0.85888	10.00085	E9, E10
CVE-2008-0015	0.85888	10.00085	E11,E12, E21, E22, E23
CVE-2009-1918	0.99968	10.00085	E13, E16
CVE-2018-7841	0.99968	6.442977	E14, E18
CVE-2004-0840	0.99968	10.00085	E15
CVE-2008-5416	0.7952	10.00085	E17, E19
CVE-2001-1030	0.99968	6.442977	E24
CVE-2009-1535	0.99968	6.442977	E25

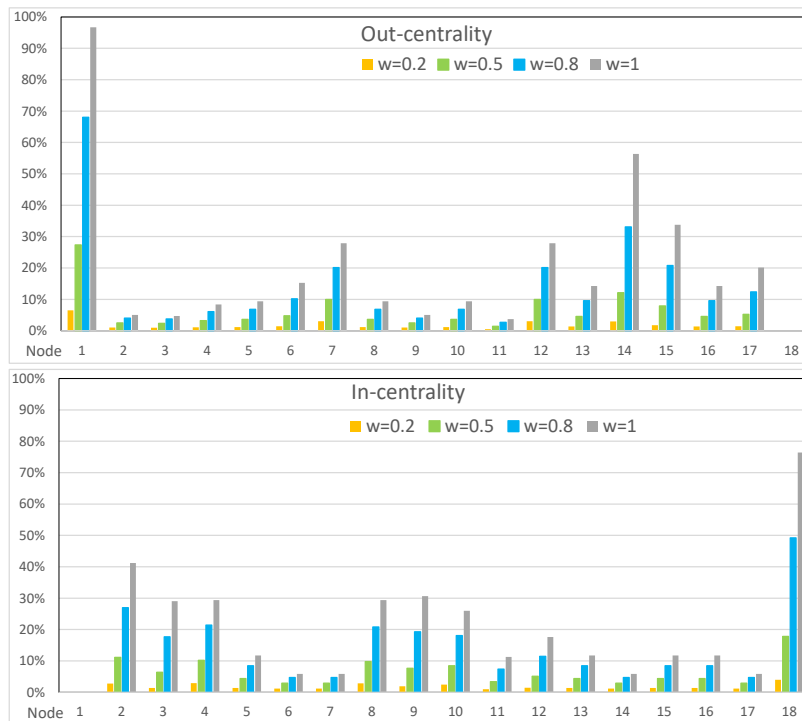


Figure 3: Out- and in-centrality values of the Multi-cloud Enterprise Network of 18 nodes in Fig. 1. The histograms show the effects of using weighted link values according to the exploitability of vulnerabilities.

values because paths originating from these nodes have many alternatives. Similarly, multiple alternative paths leading to an end node increase its in-centrality value.

When planning, the mitigation actions are optimised based on detailed network modelling and the order of actions can change depending on the exploitability or link weight values of vulnerabilities. Additionally, skilled attackers may utilise longer attack path lengths because their probability of success remains high even with multiple consecutive exploits.

Use Case 2: Netflix OSS Architecture. The second use case is a combination of containers provided by Netflix, consisting of the Spring cloud ecosystem. [21] Table 3 provides descriptions of the 21 nodes in the NetflixOSS attack graph, the topology of which is depicted in Fig. 4.

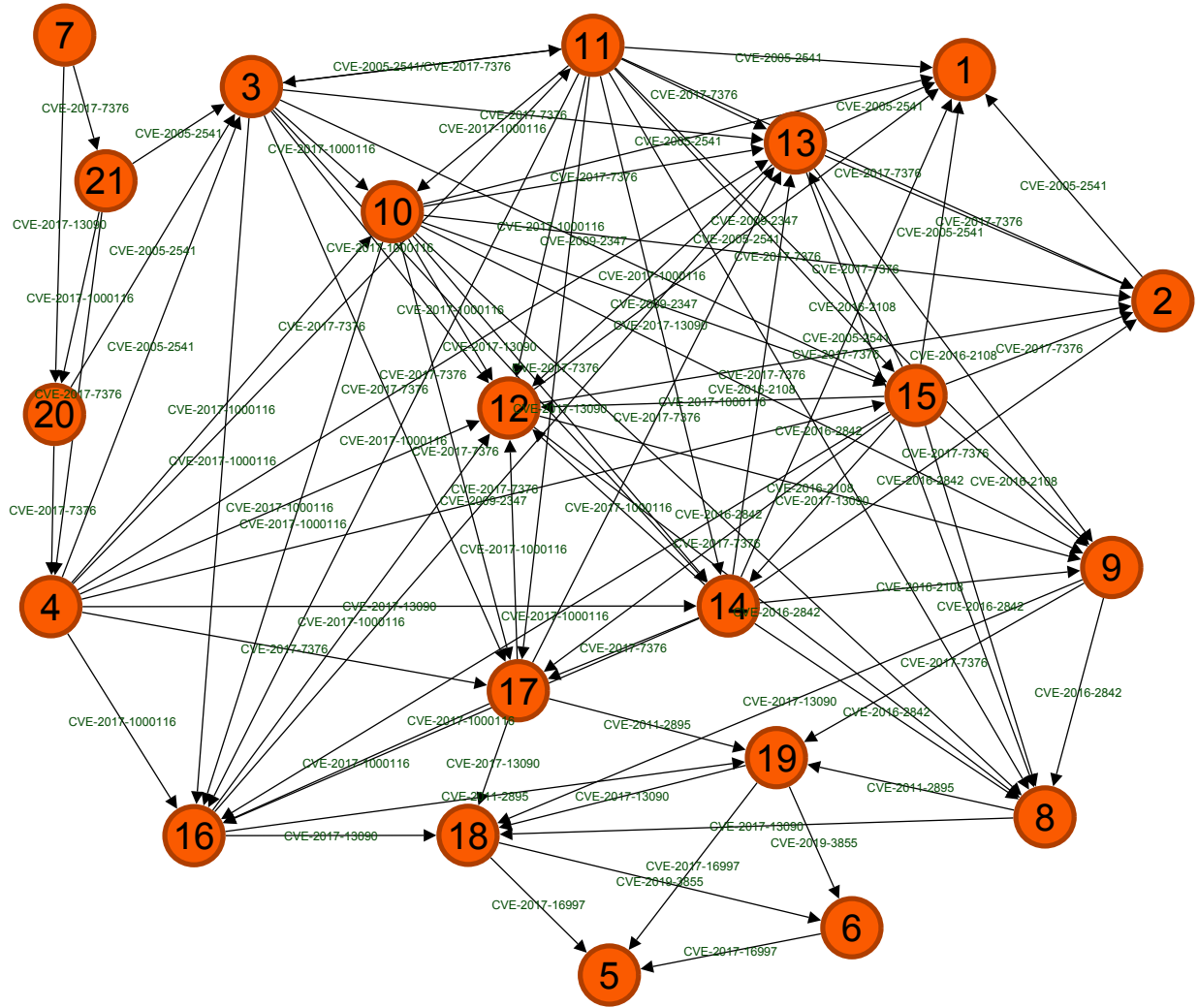


Figure 4: Use Case 2: Attack graph NetflixOSS from [21]. Nodes are described in Table 3.

In Fig. 5 we show the out-centrality and in-centrality values of the NetflixOSS Attack graph [21] for four link weight values and they are found to increase monotonically as the link weight increases. However, the growth rate is slow for low link weights, then increases, and finally slows down again with high link weights due to saturation effects. The out-centrality in Fig. ?? and in-centrality in Fig. ?? illustrate the two aspects of the NetflixOSS attack graph. The out-centrality values for the 21 nodes of the graph show that nodes 3, 4, 7, 10, 11, 20, and 21 are positioned at the beginning of possible attack chains, while nodes 1, 2, 5, 6, 8, 9, 18, and 19 are at the end of the attack chains. The node 7 is identified as the start node of the graph as it has a hundred per cent out-centrality value for the link weight values $w = 1$. Nodes 12, 13, 14, 15, 16, and 17 are in the intermediary positions within the attack chains, which can be used to prioritise protective actions or mitigate the impacts of the ongoing cyber attacks.

In Fig. 6, the average percentage of exploited nodes is shown when a node’s vulnerabilities are protected. The results are displayed for link weight values $w = 0.2$, $w = 0.5$, and $w = 0.8$ when the start node is 7. Here the effects are computed as average effects on other nodes. The dotted lines illustrate the average percentage of exploited nodes when the nodes are not protected. The relationship between the link weights of the nodes and the average effect on the network is not linear. For instance, the link weight of $w = 0.2$ results in only about 10 per cent exploitation in the network. Meanwhile, the link weights of $w = 0.5$ and $w = 0.8$ lead to approximately sixty and ninety per cent exploitation levels, respectively.

A significant decrease in the number of exploited nodes is seen when we protect the vulnerabilities of the nodes 3, 4, 20, and 21 in the graph. This is expected because these nodes are at the beginning of potential attack chains starting from

Table 3: List of nodes in the NetflixOSS attack graph in Fig.4.

Node	Description	Node	Description
1	Config service (Admin priv)	12	Service b (Admin priv)
2	Config service (User priv)	13	Service b (User priv)
3	Eureka (Admin priv)	14	Service c (Admin priv)
4	Eureka (User priv)	15	Service c (User priv)
5	Hystrix dashboard (Admin priv)	16	Spring cloud dasboard (Admin priv)
6	Hystrix dashboard (User priv)	17	Spring cloud dasboard (User priv)
7	Outside (Admin priv)	18	Turbine (Admin priv)
8	rabbitmq (Admin priv)	19	Turbine (User priv)
9	rabbitmq (User priv)	20	Zuul (Admin priv)
10	Service (Admin priv)	21	Zuul (User priv)
11	Service (User priv)		



Figure 5: Out-centrality and in-centrality values for the 21 nodes of the NetflixOSS example network network in Fig.4 for four different link weight values.

node 7. The impact is bigger when the links have higher weights. Nodes that come right after the start node become more important as the link weight values (exploitability) increase.

When it comes to addressing vulnerabilities, it may be more useful to focus on eliminating vulnerabilities related to services rather than just protecting individual nodes in the attack graph. Next, we compare how the out-centrality and in-centrality values decrease when vulnerabilities in the services are protected. The comparison will be performed by taking the difference between the unprotected and protected results. Fig. 7 shows these differences (i.e. decrease) for nodes 1 – 21 after protecting all the vulnerabilities in the services indicated in the legend. For this example, the link weight is $w = 0.8$ to represent a skilled perpetrator. Looking at the out-centrality histogram in Fig. ??, we observe that four bars stand out: Zuul and Eureka have decreased by 95% and 85% for node 7 out-centrality, and Eureka also shows a significant decrease for node 20 (85%) and for node 21 (88%) out-centrality values.

The in-centrality values shown in Fig. ?? indicate that protecting services in the nodes leads to a decrease in the in-centrality values of those particular nodes. For example, Turbine services have a significant impact on nodes 18 and 19. Additionally, protecting the Turbine services results in a substantial decrease in the in-centrality values of nodes 5

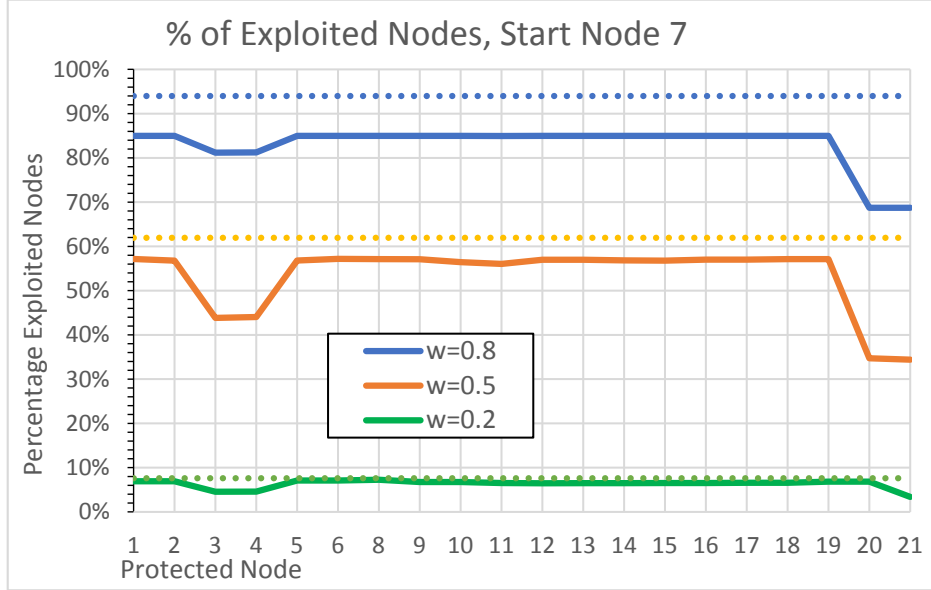


Figure 6: The average percentage values of exploited nodes in the NetflixOSS example network in Fig. 4 when a node is protected. The results are shown for link weight values of $w = 0.2$, $w = 0.5$, and $w = 0.8$. The start node of the attack is 7. The effects are calculated as average effects on other nodes. The dotted lines show the average percentage of exploited nodes when nodes are not protected.

and 6. Conversely, protecting services at the beginning of attack chains, such as Zuul and Eureka services, affect the in-centrality values of nodes 3 and 4. Services exploited later in the attack chains have no effects on these nodes.

Fig. 8a illustrates the decrease of the in-centrality values from the start node 7 to other nodes in the graph for the link weight of $w = 0.8$ after protecting a vulnerability indicated on the horizontal axis. In the model (see Section 2) these correspond to decrease in the matrix element values $C(s, t)$, for $s = 7$ and $t = 1, 2, 3, 4, 5, 6, 8, \dots, N$. By protecting the vulnerabilities CVE-2017-7376 and CVE-2017-13090, a significant decrease in the in-centrality values for several nodes can be achieved. Results at the node level indicate that CVE-2017-7376 affects significantly the in-centralities of nodes 1, 2, 4, 11, 13, 17, and 21, with smaller effects on the other nodes. On the other hand, the vulnerability CVE-2017-13090 has a major impact on nodes 14 and 18, but with minor effects on the other nodes.

Fig. 8b illustrates the decrease in the in-centrality values from the start node 7 to other nodes in the graph for the link weight of $w = 0.8$ after protecting vulnerabilities in the services indicated on the horizontal axis. Zuul and Eureka are the most effective services to be protected as they are at the beginning of attack chains. In Fig. 9a we show the summary of the decrease in the average out-centrality from the start node 7 to other nodes for the link weight $w = 0.8$ after protecting the vulnerabilities. The four most important vulnerabilities in this order are CVE-2017-7376, CVE-2017-13090, CVE-2017-1000116, and CVE-2005-2541. Fig. 9b shows the corresponding results for the services. The most important services are Zuul and Eureka as we have already seen in Fig. 8b.

Use Case 3: Pony APT campaign. The third use case involves an attack graph generated in [3] using an attack investigation tool. This tool integrates natural language processing and deep learning techniques into data analysis to model sequence-based attack and non-attack entities.

Fig. 10 depicts attack and non-attack entities detected by the ATLAS investigation tool [3]. The original attack entities are indicated by the red colour and the original non-attack by the green colour. [3] The blue line shows the extended set of attack nodes reachable from start nodes 8 or 9 by following all alternative paths in the graph. The red line shows the minimum set of nodes restricted to the original set of attack nodes.

In Fig. 11 we show the out- and in-centrality values for the 39 nodes of the ATLAS causal graph for four different link weight values. The histograms in Fig. 11 are similar to those in Fig. 5, but there are some differences. When comparing the ATLAS and NetflixOSS graphs, we can observe that the out-centrality and in-centrality values for the ATLAS causal graph for low link weight values are much smaller. Additionally, the centrality values for higher link weight values are roughly half of the Netflix results. These differences are attributed to the higher density and higher mean node degree of the NetflixOSS graph compared to the ATLAS graph.

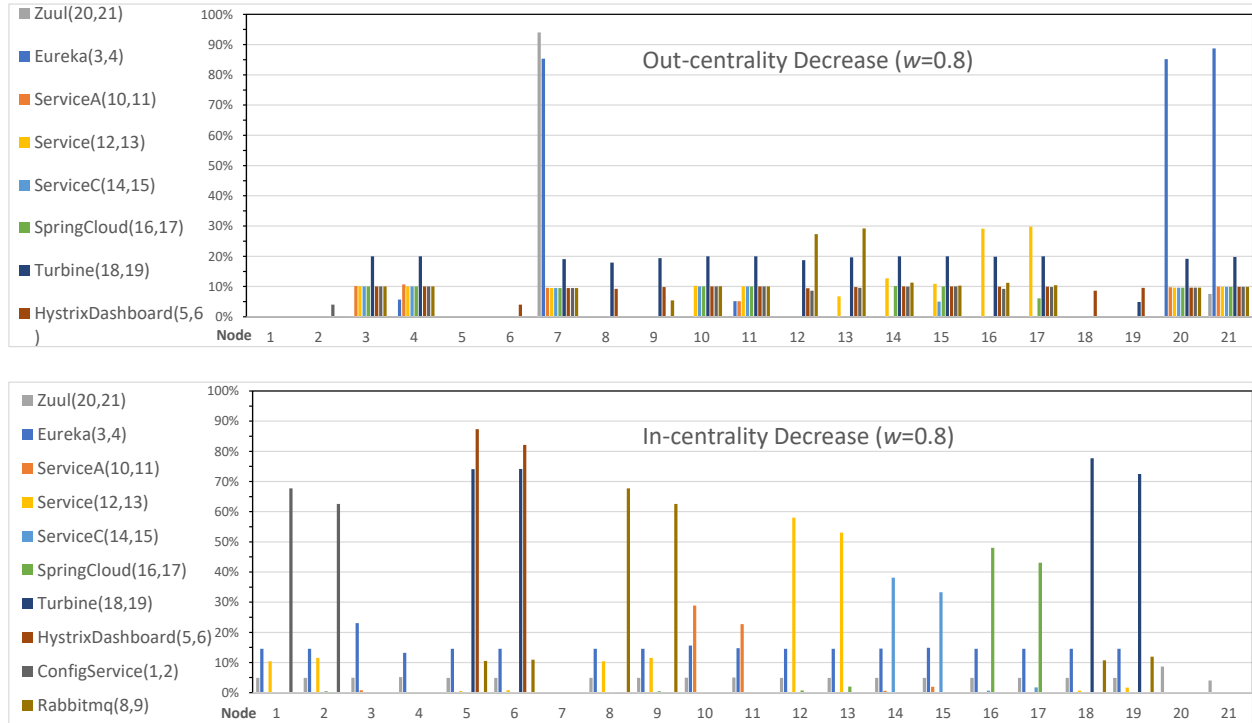
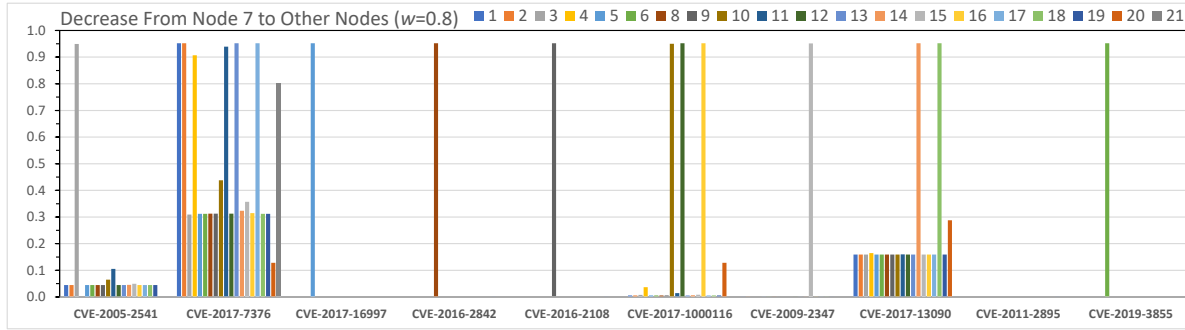


Figure 7: Out-centrality and in-centrality differences (i.e. decrease) for nodes 1 to 21 in Fig. 4 after protecting vulnerabilities in services indicated in the legend (link weight $w = 0.8$) and the start node of attack being 7.

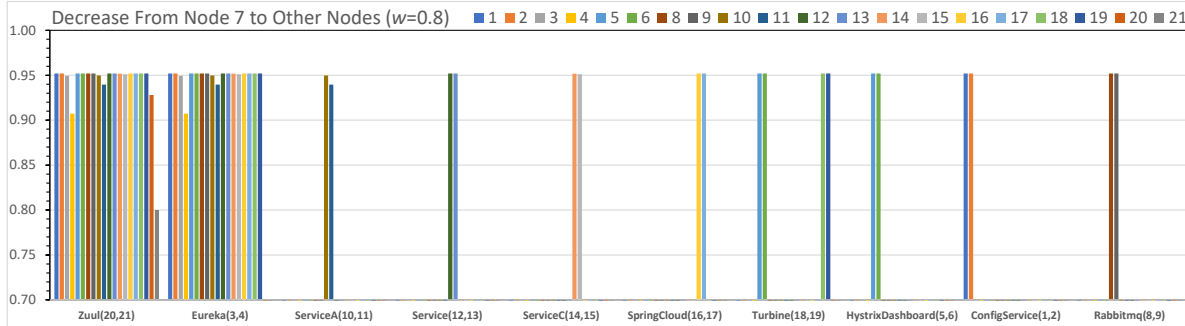
Fig. 12 illustrates the percentage of exploited nodes in the ATLAS causal graph when one of the 39 nodes is protected. The results are presented for three link weight values: $w = 0.2$, $w = 0.5$, and $w = 0.8$. The start node is node 8 or node 9. The effects are calculated as average values on the other nodes. The dotted lines represent the average percentage of the exploited nodes when no nodes are protected. Compared to Fig. 6 results, we observe more fluctuations but with lower amplitude. Removing vulnerabilities in the nodes 5, 11, 15, 21, and 33 have the highest effects in mitigating the attack. Just like in the case of Fig. 11, the lower density causes the curves to be lower compared to those of Fig. 6, and the interrelationship between the curves turn out to be different.

In contrast to the networks in use cases 1 and 2, the ATLAS causal graph (Fig. 10) has a loop between the nodes 15, 22, and 24, and bidirectional links between the nodes 10 and 11, and between the nodes 30 and 31. To apply our model, we assume that due to a loop and bidirectionality, circular and recurrent effects are possible. Fig. 13 illustrates circular effects in the ATLAS causal graph for three different link weight values. The histogram show a difference between two situations, namely one with circular effect, and the other with only self-avoiding paths in the network structure. The effects vary based on the link weight values. They are low when the link weights are $w = 0.2$, peak at higher link weights, and gradually slow down due to saturation effects for high link weight values.

To summarise it turns out that for the attack graph with one loop and two bidirectional links the out-centrality values are increased. Furthermore, nodes 1, 2, 8, and 9 have increasing out-centrality values because they are in the beginning of attack paths that can reach those nodes. Upon examining the graph in Fig.12, we conclude that the in-centrality values of nodes 5, 7, 10, 11, 12, 13, and 23 have increased due to the circular effects by the loop and the in-centrality values of nodes 28 and 33 have increased due to the recurrent effects between nodes 30 and 33 by the two bidirectional links.

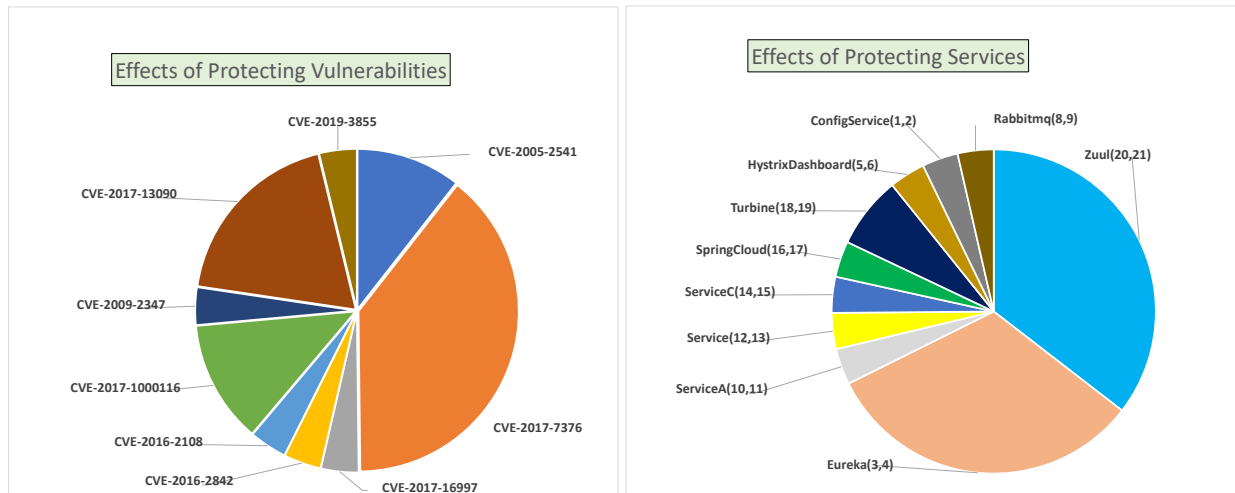


(a) Differences (i.e. decrease) of the in-centrality from the attack start node 7 to other nodes (link weight $w = 0.8$) after protecting a vulnerability from the network. Vulnerabilities are indicated on the horizontal axis.



(b) Differences (i.e. decrease) of the in-centrality from the attack start node 7 to other nodes (link weight $w = 0.8$) after removing all vulnerabilities from a server. Servers are indicated on the horizontal axis.

Figure 8: Summaries generated from the model (a) when the entire network is protected against a single vulnerability or (b) a server is protected against all its vulnerabilities.



(a) A specific vulnerability protected from the attack graph indicated on the legend (Summary from Fig. 8a). (b) Vulnerabilities protected from specific servers/services indicated on legend (Summary from Fig. 8b).

Figure 9: Relative effects after protecting a vulnerability from the network or all vulnerabilities from a server. As an example, the results are shown for the link weight value $w = 0.8$.

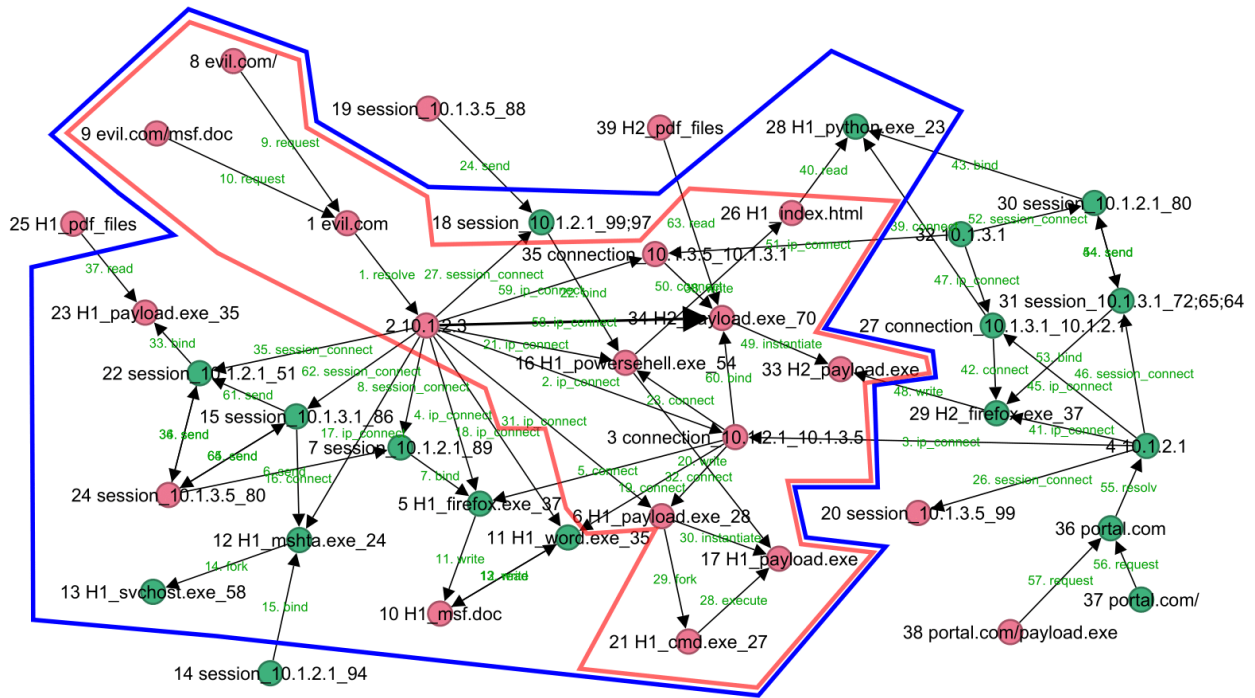


Figure 10: Use Case 3: Attack entities predicted from the connections in the graph structure. The original attack entities are indicated by the red colour and the original non-attack by the green colour. [3] The blue line shows the extended set of attack nodes detected by our network modelling method, and the red line shows the minimum set of reachable nodes restricted to the original set of attack nodes.



Figure 11: Out-centrality and in-centrality values for the 39 nodes of the ATLAS causal graph in Fig.10 for four different link weight values.

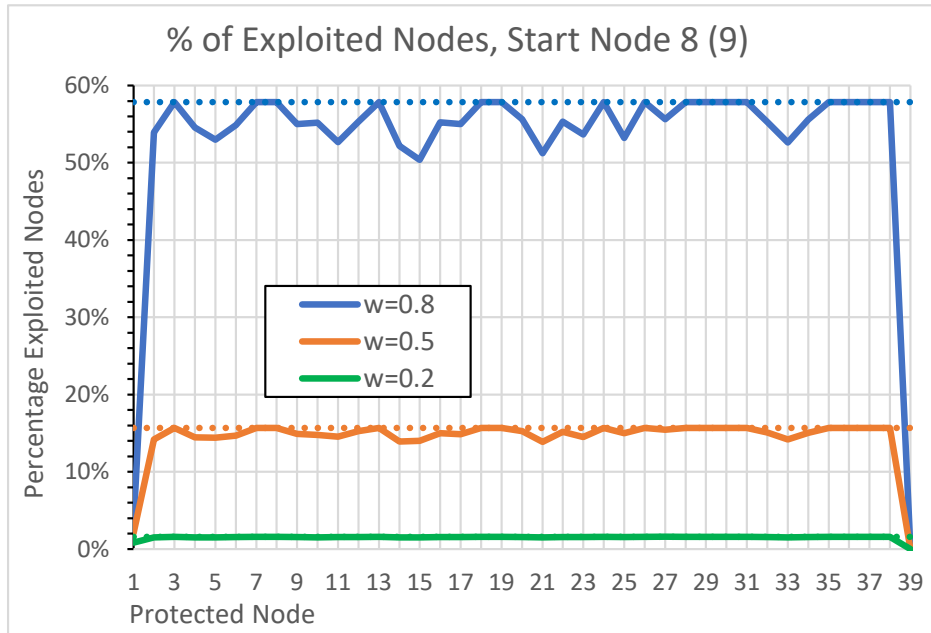


Figure 12: The average percentage values of exploited nodes in the ATLAS causal graph in Fig. 10 when a node is protected. The results are shown for the link weight values $w = 0.2$, $w = 0.5$, and $w = 0.8$. The start node is 8 or 9. The effects are calculated as average effects on other nodes. The dotted lines show the average percentage values of exploited nodes when nodes are not protected.

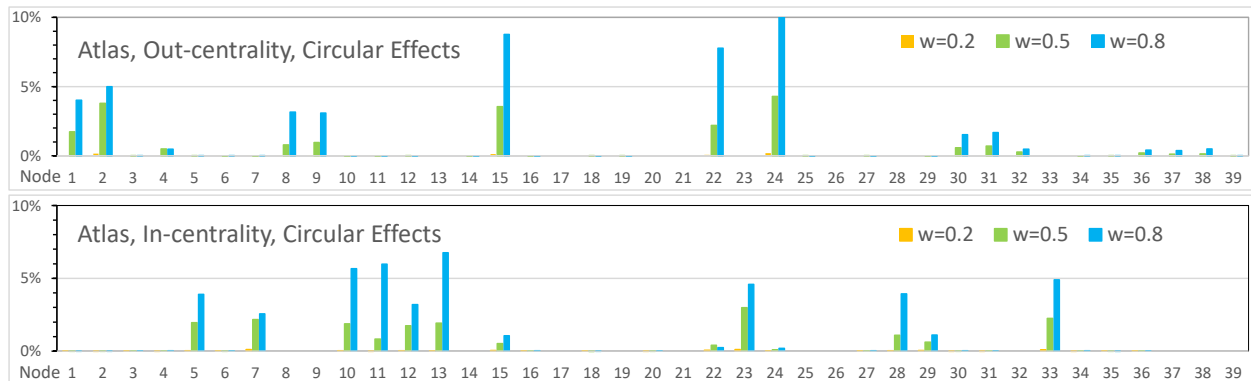


Figure 13: Circular Effects in the ATLAS causal graph of Fig.10 for three different link weight values. The bars in the histograms show differences between two calculations: full breakthrough propagation and self-avoiding paths between nodes.

5 Concluding Remarks

Cyber-related graphs, such as attack graphs, have traditionally been created manually or generated by scanning network configurations to identify vulnerabilities and compute potential attack paths. Typically, analysing attack graphs involves examining individual paths that an attacker might take and evaluating the risk associated with each path.

The use case data we analysed in this study had undergone several preprocessing steps. Future research should investigate how each preprocessing step affects the validity and semantic interpretation of the attack propagation process in real-world contexts. Additionally, multiplex network representations should be used to investigate the roles and effects of different node classes within attack graphs.

In this study, we have introduced probabilistic methods for analysing attack graphs or causal graphs. These methods have previously been used in our research to model the spread of influence in complex networks. Here, we are applying this methodology for the first time to analyse the propagation of the attack.

In this context out-centrality and in-centrality measures are used to identify critical nodes in the graph. The documented exploitability values of vulnerabilities mimic the probability of propagation of attacks on possible paths or sequences of actions that an attacker can follow to achieve a particular objective, such as compromising a critical asset in a network. Similarly, the documented impact values of vulnerabilities are used to demonstrate the model in analysing cumulative and individual impacts of attacks.

In summary we have developed a novel method for analysing alternative paths within an attack graph and calculating their combined exploitability and impact. This approach differs from the previous methods, since our approach offers a probabilistic framework to assess the combined effects of the entire attack graph, rather than focusing solely on the maximum or minimum scenarios. We have applied our model by presenting results related to functional services based on identified vulnerabilities. Additionally, this method can be extended to analyse multiple attack graphs simultaneously in a network structure. For higher levels of abstraction and summaries, it is essential to aggregate alternative paths within the model consistently. This integrated perspective improves understanding of the situation and helps prioritise mitigation efforts.

Data Availability

The datasets utilised in this article have been obtained from open online sources. The respective datasets and graphs have been provided by authors of the referenced original articles [21, 8, 3].

References

- [1] M. Ugur Aksu et al. “Automated Generation of Attack Graphs Using NVD”. In: CODASPY ’18. New York, NY, USA: Association for Computing Machinery, Mar. 2018, pp. 135–142. ISBN: 978-1-4503-5632-9. DOI: 10.1145/3176258.3176339. (Visited on 09/29/2024).
- [2] Into Almiala, Henrik Aalto, and Vesa Kuikka. “Influence spreading model for partial breakthrough effects on complex networks”. In: *Physica A: Statistical Mechanics and its Applications* 630 (2023), p. 129244. DOI: <https://doi.org/10.1016/j.physa.2023.129244>.
- [3] Abdullellah Alsaheel et al. “{ATLAS}: A sequence-based learning approach for attack investigation”. In: *30th USENIX security symposium (USENIX security 21)*. 2021, pp. 3005–3022. URL: <https://www.usenix.org/conference/usenixsecurity21/presentation/alsaheel>.
- [4] Faeiz M Alserhani. “Knowledge-based model to represent security information and reason about multi-stage attacks”. In: *Advanced Information Systems Engineering Workshops: CAiSE 2015 International Workshops, Stockholm, Sweden, June 8-9, 2015, Proceedings 27*. Springer, 2015, pp. 482–494. DOI: https://doi.org/10.1007/978-3-319-19243-7_44.
- [5] Genwei Jiang et al. *CVE-2017-0199: In the Wild Attacks Leveraging HTA Handler | Mandiant*. <https://cloud.google.com/blog/topics/threat-intelligence/cve-2017-0199-hta-handler>. (Visited on 07/30/2024).
- [6] Md Ariful Haque et al. “Realizing cyber-physical systems resilience frameworks and security practices”. In: *Security in Cyber-Physical Systems: Foundations and Applications* (2021), pp. 1–37. DOI: https://doi.org/10.1007/978-3-030-67361-1_1.
- [7] Eric M Hutchins, Michael J Cloppert, Rohan M Amin, et al. “Intelligence-driven computer network defense informed by analysis of adversary campaigns and intrusion kill chains”. In: *Leading Issues in Information Warfare & Security Research* 1.1 (2011), pp. 112–125.

- [8] Amjad Ibrahim, Stevica Bozhinoski, and Alexander Pretschner. “Attack Graph Generation for Microservice Architecture”. In: *Proceedings of the 34th ACM/SIGAPP Symposium on Applied Computing*. Limassol Cyprus: ACM, Apr. 2019, pp. 1235–1242. ISBN: 978-1-4503-5933-7. DOI: [10.1145/3297280.3297401](https://doi.org/10.1145/3297280.3297401). (Visited on 07/02/2024).
- [9] B Kordy, L Piètre-Cambacédès, and P Schweitzer. *DAG-based attack and defense modeling: don’t miss the forest for the attack trees*. *Comput. Sci. Rev.* 13–14, 1–38 (2014). DOI: <https://doi.org/10.1016/j.cosrev.2014.07.001>.
- [10] Vesa Kuikka and Kimmo K. Kaski. “Detailed-level modelling of influence spreading on complex networks”. In: *Scientific Reports* 14.28069 (2024). DOI: <https://doi.org/10.1038/s41598-024-79182-9>.
- [11] Vesa Kuikka et al. “Efficiency of Algorithms for Computing Influence and Information Spreading on Social Networks”. In: *Algorithms* 15.8 (2022). ISSN: 1999-4893. DOI: <http://dx.doi.org/10.3390/a15080262>.
- [12] Harjinder Singh Lallie, Kurt Debattista, and Jay Bal. “A review of attack graph and attack tree visual syntax in cyber security”. In: *Computer Science Review* 35 (2020), p. 100219. DOI: <https://doi.org/10.1016/j.cosrev.2019.100219>.
- [13] Andrea Landherr, Bettina Friedl, and Julia Heidemann. “A Critical Review of Centrality Measures in Social Networks”. In: *Business & Information Systems Engineering* 2.6 (2010), pp. 371–385. DOI: <https://doi.org/10.1007/s12599-010-0127-3>.
- [14] Yuchong Li and Qinghui Liu. “A comprehensive review study of cyber-attacks and cyber security; Emerging trends and recent developments”. In: *Energy Reports* 7 (2021), pp. 8176–8186. DOI: <https://doi.org/10.1016/j.egyrs.2021.08.126>.
- [15] Changwei Liu, Anoop Singhal, and Duminda Wijesekera. “Using attack graphs in forensic examinations”. In: *2012 Seventh International Conference on Availability, Reliability and Security*. IEEE. 2012, pp. 596–603. DOI: <https://doi.org/10.1109/ARES.2012.58>.
- [16] Peter Mell, Karen Scarfone, and Sasha Romanosky. *A Complete Guide to the Common Vulnerability Scoring System Version 2.0*. en. July 30, 2007. URL: https://tsapps.nist.gov/publication/get_pdf.cfm?pub_id=51198.
- [17] Yulu Qi et al. “Cybersecurity knowledge graph enabled attack chain detection for cyber-physical systems”. In: *Computers and Electrical Engineering* 108 (2023), p. 108660. DOI: <https://doi.org/10.1016/j.compeleceng.2023.108660>.
- [18] Mariana Segovia-Ferreira et al. “A Survey on Cyber-Resilience Approaches for Cyber-Physical Systems”. In: *ACM Computing Surveys* 56.8 (2024), pp. 1–37. DOI: <https://doi.org/10.1145/365295>.
- [19] Oleg Sheyner and Jeannette Wing. “Tools for generating and analyzing attack graphs”. In: *International symposium on formal methods for components and objects*. Springer. 2003, pp. 344–371. DOI: https://doi.org/10.1007/978-3-540-30101-1_17.
- [20] Leslie F Sikos. “Cybersecurity knowledge graphs”. In: *Knowledge and Information Systems* 65.9 (2023), pp. 3511–3531. DOI: <https://doi.org/10.1007/s10115-023-01860-3>.
- [21] George Stergiopoulos, Panagiotis Dedousis, and Dimitris Gritzalis. “Automatic analysis of attack graphs for risk mitigation and prioritization on large-scale and complex networks in Industry 4.0”. In: *International Journal of Information Security* 21.1 (2022), pp. 37–59. DOI: <https://doi.org/10.1007/s10207-020-00533-4>.
- [22] Branka Stojanović, Katharina Hofer-Schmitz, and Ulrike Kleb. “APT datasets and attack modeling for automated detection methods: A review”. In: *Computers & Security* 92 (2020), p. 101734. DOI: <https://doi.org/10.1016/j.cose.2020.101734>.
- [23] Jasmin Wachter. *Graph Models for Cybersecurity – A Survey*. Nov. 2023. arXiv: 2311.10050 [cs]. (Visited on 08/02/2024).
- [24] Lingyu Wang et al. “An attack graph-based probabilistic security metric”. In: *Data and Applications Security XXII: 22nd Annual IFIP WG 11.3 Working Conference on Data and Applications Security London, UK, July 13-16, 2008 Proceedings* 22. Springer. 2008, pp. 283–296. DOI: https://doi.org/10.1007/978-3-540-70567-3_22.
- [25] Kengo Zenitani. “Attack graph analysis: an explanatory guide”. In: *Computers & Security* 126 (2023), p. 103081. DOI: <https://doi.org/10.1016/j.cose.2022.103081>.